



Broadband classification of spherical shells in a waveguide

*John A. Fawcett
Jüri Sildam*

Defence R&D Canada – Atlantic

Technical Memorandum
DRDC Atlantic TM 2008-217
November 2008

This page intentionally left blank.

Broadband classification of spherical shells in a waveguide

John A. Fawcett
Jüri Sildam

Defence R&D Canada – Atlantic

Technical Memorandum

DRDC Atlantic TM 2008-217

November 2008

Principal Author

Original signed by John Fawcett

John Fawcett

Approved by

Original signed by David Hopkin

David Hopkin
Head/Maritime Asset Protection

Approved for release by

Original signed by Ron Kuwahara for

Calvin Hyatt
Head/Document Review Panel

© Her Majesty the Queen in Right of Canada as represented by the Minister of National Defence, 2008

© Sa Majesté la Reine (en droit du Canada), telle que représentée par le ministre de la Défense nationale, 2008

Abstract

In this paper, a multipath expansion method is used to model the scattering from a large set of spheres in a Pekeris waveguide. The spherical shells have different radii, relative thicknesses, and three different materials and are grouped into 6 classes: thick and thin-shelled and 3 different material compositions. The classification of the spheres from their echos is considered, first for the sphere in free space and then for the spheres in the waveguide. The cross-correlations of the observed echos with a library of echos is the basis of the classification. In the case of echos from a sphere in a waveguide, we consider the resulting classifications when using a library of free space echos and then echos modified with increasing accuracy to account for the waveguide propagation. The cross-correlation based classification approach has been chosen because of its common use in sonar target detection applications. It is hoped that the present results can be used as an intuitive baseline for the development of other target/waveguide classification methods.

Résumé

Dans cet article, une méthode de développement des trajets multiples est utilisée pour modéliser la diffusion dans un guide d'onde de Pekeris d'un grand ensemble de sphères. Les coquilles sphériques ont différents rayons et différentes épaisseurs relatives, et elles sont faites de trois matériaux distincts. Elles sont groupées en 6 classes, selon l'épaisseur de leur paroi (épaisse ou mince) et le matériau dont elles sont faites (trois possibilités). La classification des sphères au moyen de leurs échos est étudiée, d'abord pour les sphères en espace libre, puis pour les sphères dans un guide d'onde. La corrélation croisée des échos observés avec des échos provenant d'une bibliothèque sert de base à la classification. Dans le cas des échos provenant d'une sphère dans un guide d'onde, nous étudions la classification obtenue avec une bibliothèque d'échos en espace libre, puis avec des échos modifiés avec de plus en plus de précision pour tenir compte de la propagation dans le guide d'onde. L'approche de classification au moyen de la corrélation croisée a été choisie parce qu'elle est souvent utilisée pour la détection de cibles sonar. Nous espérons que les résultats de cette étude pourront servir de base intuitive pour le développement d'autres méthodes de classification cible/guide d'onde.

This page intentionally left blank.

Executive summary

Broadband classification of spherical shells in a waveguide

John A. Fawcett, Jüri Sildam; DRDC Atlantic TM 2008-217; Defence R&D Canada – Atlantic; November 2008.

Background: The detection and classification of a sonar echo is a problem of much interest for many sonar applications: for example, ASW, torpedo defence, minehunting and diver detection. Underwater objects may be classified from their broadband backscattered spectra or echos. However, when the object is located within a waveguide, the combinations of the various multipaths may affect the resultant received signal and complicate the classification problem. In this report, a large set of echos for spheres of differing sizes, shell thicknesses, and material compositions is generated, both for the spheres in free space and in a waveguide for the spheres at various specified depths and ranges. The classification of these echos is considered. Various cases are considered: classification when both the testing and training sets consist of free-space echos, classification when the testing set consists of waveguide echos and the training set consists of free-space echos and finally when a set of approximate or exact waveguide echos is computed for the training set.

Principal results: It was found that good classification results were obtained when the echos used for both the training and testing sets were from free space. In a waveguide situation, if the separation of the direct and other multipath arrivals are sufficiently separated in time then good classification results are obtained when using the free space echos in the training set. If the target is distant or the source/receiver or target is close to the upper surface or seabed, then the free space echos will, in general, not classify targets well. In this case, echos corresponding to a position close to the target's true position need to be computed. This can be done by jointly classifying the target and searching over a set of hypothesized positions. The method described in this paper is robust with respect to reverberation noise due to the coherent matched filtering which is used.

Significance of results: The paper shows that it is possible to classify objects in a waveguide from their wideband echos. Although spheres were considered in this report for computational efficiency the same approach could be used for a database of more general targets' echos. A wideband echo classification system could be used in conjunction with ASW, minehunting or diver detection sonar systems. In the case that the echos from the objects are not affected significantly from multipath interference effects (e.g. free space echos or a deep waveguide) then the resulting

classification performance can be very good. However, in many shallow waveguide scenarios good classification performance may depend upon generating target echos in the classifier database for a set of hypothesized target positions which are sufficiently close to the true target position. Using a simultaneous position estimation and target classification approach, good classification results can be obtained. The results of this report lead to a better understanding of the problem of target detection in a waveguide and can be used as a baseline for the development of new classification methods for the target/waveguide detection problem.

Future work: We are continuing to investigate the efficient numerical generation of target echos for varying target positions in the waveguide. We would also like to investigate improving waveguide classification performance by the use of additional source/receivers or different feature sets. In order to determine the practical classification performance of methods, it would be very useful to obtain experimental broadband scattering data for more general target shapes in a realistic underwater setting.

Sommaire

Broadband classification of spherical shells in a waveguide

John A. Fawcett, Jüri Sildam ; DRDC Atlantic TM 2008-217 ; R & D pour la défense Canada – Atlantique ; novembre 2008.

Introduction : La détection et la classification des échos sonar présente un intérêt considérable pour de nombreuses applications sonar, comme la GASM, la défense contre les torpilles, le déminage et la détection des plongeurs. Les objets sous-marins peuvent être classés selon leur spectre rétrodiffusé large bande (leurs échos). Cependant, quand un objet est situé dans un guide d'onde, la combinaison des rayons sonores ayant suivi des trajets différents peut brouiller le signal reçu et compliquer la classification. On a généré un grand ensemble d'échos de sphères dont la taille, l'épaisseur de la paroi et le matériau varient. Certaines sphères sont situées en espace libre, d'autres dans un guide d'onde, à différentes profondeurs et distances. La classification de ces échos est étudiée. Divers cas sont examinés : la classification lorsque les ensembles d'essai et d'apprentissage sont composés d'échos en espace libre, lorsque l'ensemble d'essai est composé d'échos dans un guide d'onde et l'ensemble d'apprentissage d'échos en espace libre, et enfin lorsque des échos dans un guide d'onde sont calculés exactement ou approximativement pour créer l'ensemble d'apprentissage.

Résultats : De bons résultats de classification ont été obtenus lorsque les échos utilisés pour les ensembles d'essai et d'apprentissage étaient en espace libre. Dans un guide d'onde, si l'écho principal est suffisamment séparé dans le temps des échos ayant suivi d'autres trajets, on obtient de bons résultats de classification en utilisant les échos en espace libre comme ensemble d'apprentissage. Si la cible est lointaine, ou encore si la cible ou le récepteur est situé près de la surface ou du fond, l'utilisation des échos en espace libre ne permettra généralement pas de bien classer les cibles. Dans ce cas, il faut calculer des échos qui correspondent à une position proche de la position réelle de la cible. On peut faire ce calcul en effectuant en même temps la classification de la cible et une recherche dans un ensemble de positions hypothétiques. La méthode décrite dans cet article est résistante à l'égard du bruit de réverbération grâce à l'utilisation d'un filtrage cohérent adapté.

Portée : Cet article démontre qu'il est possible de classer les objets dans un guide d'onde au moyen de leurs échos large bande. Bien qu'on ait étudié des sphères pour des raisons d'économie de calcul, la même approche pourrait être utilisée avec une base de données d'échos de cibles de formes plus générales. Un système de classification d'échos large bande pourrait être utilisé conjointement avec des systèmes sonar

de GASM, de déminage ou de détection des plongeurs. Dans le cas où les échos des objets ne sont pas perturbés par d'importants effets de brouillage dû aux trajets multiples (dans l'espace libre ou dans un guide d'onde profond), on peut obtenir un très bon rendement de classification. Cependant, dans bien des scénarios de guide d'onde peu profond, il peut être nécessaire de générer des échos pour un ensemble de positions hypothétiques de la cible suffisamment proches de sa position réelle et d'ajouter ces échos à la base de données du classificateur pour arriver à de bons résultats. Il est possible d'obtenir un bon rendement en utilisant une approche simultanée d'estimation de la position et de classification de la cible. Les résultats de ce rapport améliorent la compréhension du problème de la classification dans un guide d'onde et peuvent être utilisés comme base pour le développement de nouvelles méthodes de classification pour le problème de détection cible/guide d'onde.

Travaux futurs : Nous continuons de chercher des méthodes économiques de génération numérique d'échos pour différentes positions de la cible dans le guide d'onde. Nous aimerions également faire des recherches sur la façon d'améliorer la classification dans un guide d'onde en utilisant des sources/récepteurs supplémentaires ou d'autres ensembles de caractéristiques. Pour déterminer le rendement de classification des méthodes en pratique, il serait très utile d'obtenir des données expérimentales de diffusion large bande pour des formes de cibles plus générales dans un environnement sous-marin réaliste.

Table of contents

Abstract	i
Résumé	i
Executive summary	iii
Sommaire	v
Table of contents	vii
List of figures	viii
1 INTRODUCTION	1
2 GENERATION OF BACKSCATTERED SPECTRA AND TIMESERIES	4
3 CLASSIFICATION PERFORMANCE	7
3.1 Free space classification of echos	7
3.2 Classification in a waveguide	11
4 SUMMARY	20
References	24

List of figures

Figure 1:	The 10 and 4 msec Chirp signals used in the computations	5
Figure 2:	The spectra for the 3 different material types and the echo time series for the 10-ms[2 18] kHz pulse incident upon 5.2% thick shells.	5
Figure 3:	The spectra for the 3 different material types and the echo time series for the 4-ms pulse [2 10]kHz incident upon 5.2% thick shells.	6
Figure 4:	The Confusion matrices resulting from using for the 10-msec and 4-msec Chirp pulses	8
Figure 5:	Representative 10-msec and 4-msec Chirp pulse echos with added noise for the 5.2% steel-shelled sphere.	9
Figure 6:	The Confusion matrices resulting from using for the 10-msec and 4-msec Chirp pulses with added noise.	9
Figure 7:	[top] The predicted thickness (logarithm) as a function of the true value. The mean over 4 partitions is shown with the \pm standard deviations also indicated. [bottom] The same as the top plot but noise sequences as in Fig.5 has been added to the testing set	10
Figure 8:	First column: The time series for a steel-shelled (empty) and steel-shelled (resin) at 1 m depth and 100 m range. The source/receiver are at 15m depth in a 30m deep waveguide. Second column: the series resulting from the cross-correlation with the corresponding free-space echo.	12
Figure 9:	The same as above but now the spheres are at 10m depth.	12
Figure 10:	The resulting Confusion matrices for the sphere in a waveguide (30m deep) and for the indicated depths of the spheres. The source/receiver is at 15 m depth and a range of 100 m.	13
Figure 11:	[top] The Confusion matrices for the sphere at 100 m range and the source receiver at 1 m depth. The waveguide depth is 20m.	15
Figure 12:	[top] The Confusion matrices for the sphere at 100 m range and the source receiver at 1 m off the seabed. The waveguide depth is 20m.	15

Figure 13:	The Confusion matrices for the sphere at 200 m range and the source receiver at 1 m depth. The waveguide depth is 20m.	16
Figure 14:	The Confusion matrices for the sphere at 200 m range and the source receiver at 1 m off the seabed. The waveguide depth is 20m.	16
Figure 15:	The time series for a steel-shelled (10%) sphere at 100m range and 2m depth for [top] shallow source/receiver [bottom] deep source/receiver	17
Figure 16:	The short time FFT spectra for a steel-shelled (10%) sphere at 100m range and 2m depth for [top] shallow source/receiver [bottom] deep source/receiver. The power is shown in dB units.	17
Figure 17:	The ambiguity surfaces resulting from cross-correlating a specified echo (at range=100 m, depth = 3 m) with echos from different waveguide positions [left] matching with echos of same type of sphere [right] with echos from different sphere	18
Figure 18:	The Confusion matrices for the sphere at 100 m range and the source receiver at 1 m depth. Eleven replicas are generated for depths bracketing the true depth and the maximum cross-correlation is used.	21
Figure 19:	The Confusion matrices for the sphere at 100 m range and the source receiver at 1 m off the seabed. Eleven replicas are generated for depths bracketing the true depth and the maximum cross-correlation is used.	21
Figure 20:	The Confusion matrices for the sphere at 200 m range and the source receiver at 1 m depth. Eleven replicas are generated for depths bracketing the true depth and the maximum cross-correlation is used.	22
Figure 21:	The Confusion matrices for the sphere at 200 m range and the source receiver at 1 m off the seabed. Eleven replicas are generated for depths bracketing the true depth and the maximum cross-correlation is used.	22
Figure 22:	The resulting Confusion matrix for the sphere at 100 m range and 1 m depth. The source/receiver is at 1 m depth. The depth of the sphere is searched over the interval [18.45 19.45]m	23

This page intentionally left blank.

1 INTRODUCTION

Over the last few years, there has been much interest in the detection and classification of underwater targets on the basis of the spectral and/or temporal features of the received echo. This has been investigated for buried and proud mine and general target/clutter classification [1-4]. Generally, the classification of echos has two fundamental challenges. The first challenge is related to one's ability to define classes of targets (or clutter), based upon a set of features, which is robust to variations in the targets' properties. For example, one might wish to classify objects of different shape as having (or not having) a thin shell even if a particular target shape is not present in the training set. The second challenge is the mismatch which results between an echo's features and the features of the training set due to external parameters such as the surrounding environment (e.g., a waveguide). In this case, one needs to define echo features that are relatively insensitive to the environment or to account (model) for the effects of the environment when comparing an echo's features to those of the training set. It is this latter approach that we will consider in this report. In our case, the scattering object may be at an unknown depth in an oceanic waveguide. A target's location within the ocean waveguide will, in general, significantly affect its echo characteristics. For example, in Ref. 5 it was shown how the echo from an aluminum sphere on a seabed was significantly different from that expected in free-space. Thus, an understanding of the target scattering process in a waveguide is important in understanding target detection and classification in a shallow water scenario. Some of the material of this report has been presented in Ref.6. The approach of this report is most related to the work of Ref. 3. In Ref.3, the authors consider targets near the seabed and use a vertical receive array. They compensate for the waveguide effects in one of two ways: (a) they estimate some waveguide and angular parameters and approximately deconvolve the waveguide response from the echo (b) they train and test on beamformed data for a target at a particular location. The problem of this report is somewhat different. First, only a point source/receiver location is considered. Second, we use a very simple cross-correlation/nearest-neighbour classification and either ignore the effects of the waveguide or attempt to estimate the unknown depth of the target by including this unknown parameter in the classification/estimation process. We do not explicitly extract echo features but instead consider a portion of the echo as the feature vector.

In an earlier report [7] we described how to incorporate the analytical scattering solution [8] from a spherical shell in free space into the scattering solution for a sphere in a simple oceanic waveguide. In particular, the sound speed of the waveguide was taken to be constant and the waveguide was bounded above by a pressure release surface and below by a seabed. A multipath expansion/scattering model was derived and this model was shown to be accurate, as compared to an exact wavenumber integral solution for frequencies above approximately 500 Hz. This model does use

the single-scatter approximation: that is, the field which is scattered by the sphere and then is reincident upon the sphere after reflections from the waveguide interfaces is ignored. This is often a very good approximation, although in [6,7] an example is shown for the sphere very close to the upper surface, where the relative importance of the rescattering terms is significant for an interval of frequencies.

We use an existing FORTRAN numerical code to generate the scattering coefficients and the backscattered spectra for a variety of spheres in free space. In particular, evacuated spherical steel and aluminum shells of varying thicknesses and diameters will be considered. As well, the steel-shelled spheres are considered with an interior resin fill using the parameters of [9]. These spheres will be divided into 6 basic classes, relatively thin or thick shells and the 3 material types: steel-shelled (evacuated interior), aluminum-shelled (evacuated interior), and steel-shelled (resin interior). The backscattered spectra will be converted into time series using Fourier synthesis with the weighting of the source spectrum. In the classification study, these echos will be divided into training and testing sets. We will use a straightforward classification approach. An echo from the testing set will be compared to those in the training set by using the maximum cross-correlation (from a sliding-window cross-correlation) as the distance. The echo in the training set which provides the maximum cross-correlation (the training set entries are first normalized) is taken to yield the class-type of the testing set echo. The classification performance in free space will be considered. The testing set of spheres is also considered within a waveguide and the multipath model of Ref. 7 used to generate the backscattered spectra and pulses as a function of the sphere depth within the waveguide. The classification performance which results when the sphere is in the waveguide at various ranges and depths is considered. Three main classification strategies are considered: (1) classification of the sphere in the waveguide using a library or "training" set of free space replicas (2) generating approximate replicas (time series) for a set of spheres and a set of depths (we will assume that the horizontal range is known) from the free space monostatic backscattered spectra (3) generating replicas (time series) for a set of spheres and a set of depths using the multipath method with precomputed sets of scattering coefficients for the spheres as a function of frequency. The difference between the last 2 methods is that in (2) it is assumed that the backscattering amplitude and phase at non-zero scattering angles (the angle between the incident and scattered multipaths from the sphere) is equal to the monostatic value, whereas in (3) the exact multipath replica is computed. The computational cost increases from (1) to (3). The other classification approach one could use would be a full inversion method, where the various spherical and location parameters are estimated by using, for example, a simulated annealing or genetic algorithm inversion of the echo. In the method of this paper, the spheres' echos or coefficients are pre-computed for a discrete set of possible parameters (training set). This allows us to consider the classification of about 2000 free space echos in a reasonable amount of time. We have considered spherical shells to simplify the

modelling. However, the classification approach used in this report can also be used for more general target shapes. Instead of using the numerically generated monostatic freespace echos to classify in the waveguide using methods (1) or (2) outlined above, one could use measured echos. In the case of method(3), where the bistatic scattering information is required, one could use sets of measured bistatic echos, at a sufficiently fine angular spacing, to provide the necessary information.

2 GENERATION OF BACKSCATTERED SPECTRA AND TIMESERIES

The scattering of sound from a spherical shell or shelled structure can be analytically described by a series of spherical harmonics. The details of this have been described previously [7] or can be found in the literature (eg. Ref. 8). In Ref. 4 the classification of spherical and cylindrical shells as either thin or thick was considered for a wide variety of shells. In this paper, we consider a somewhat similar study. We will consider 3 basic types of spheres, steel-shelled, aluminum-shelled, and steel-shelled with an interior elastic resin fill. The fill has the parameters as detailed in [9]. The parameters are as follows: for steel, we use the parameters (compressional speed, shear speed, and density), $V_p = 5950m/s, V_s = 3240m/s$, and $\rho = 7.9g/cm^3$. For aluminum we use the values: $V_p = 6380m/s, V_s = 3100m/s$ and $\rho = 2.79g/cm^3$. The compressional and shear attenuations are zero for these 2 cases. The interior resin fill has the parameters: $V_p = 3000m/s, V_s = 1550m/s, \rho = 1.845g/cm^3$ and $\alpha_p = 0.8dB/\lambda$ and $\alpha_s = 1.8dB/\lambda$. The outer radius of each of these classes is varied from 0.2 to 0.4 m in 41 steps. The relative thickness (thickness/radius) of the shell of each class is then varied in logarithmic (base 10) 31 steps from -2 to -0.05 (or 1 to 89%). For very thick shells, the sphere resembles a solid with the properties of the shell. In total, the spectra are generated for $3 \times 41 \times 31 = 3813$ different spheres. For the classification study, we generate the response for frequencies in the interval [100, 20100] Hz with a frequency increment of 10 Hz. The spectrum for the j th sphere will be denoted as $S(f; j)$. For a specified source spectrum $I(f)$ the pulse echo is generated from,

$$P(t; j) = 2\Re\left\{\sum_{k=1}^N S(f_k; j)I(f_k) \exp(-i2\pi f_k t)\right\} \Delta f \quad (1)$$

where f_k denote the discrete computed frequencies. In fact, we can implement this by defining $S(-f_k; j) = S^*(f_k; j)$ and $I(-f_k) = I^*(f_k)$ and using a FFT implementation to compute $P(t; j)$ for discrete values of t . In Fig.1 we show the tapered 10- and 4-msec Chirp pulses ([2 18] kHz, [2 10]Khz) that we will use in our computations.

In Figs.2 and 3 we show the backscattered spectra (weighted by the amplitude of the source spectrum) for the 10 and 4-msec Chirps and the corresponding time series. The free space source/receiver was located 100 m away from the sphere. The results are shown for a shell thickness of 5.2% for the steel, aluminum and steel/resin-filled spheres.

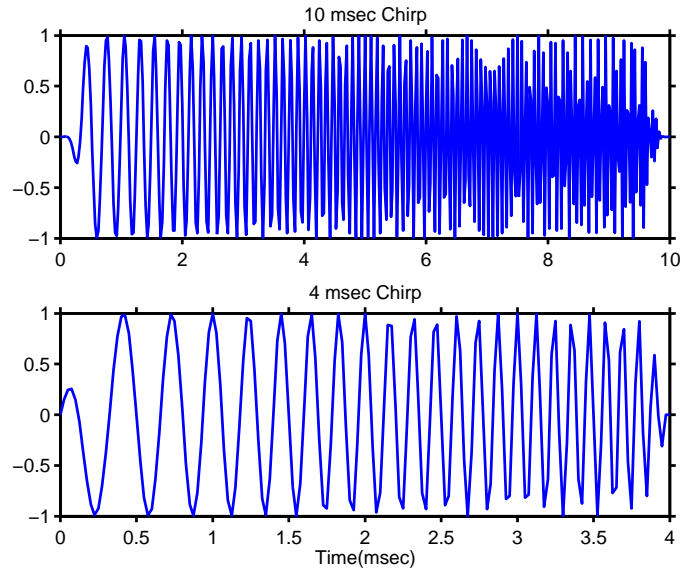


Figure 1: The 10 and 4 msec Chirp signals used in the computations

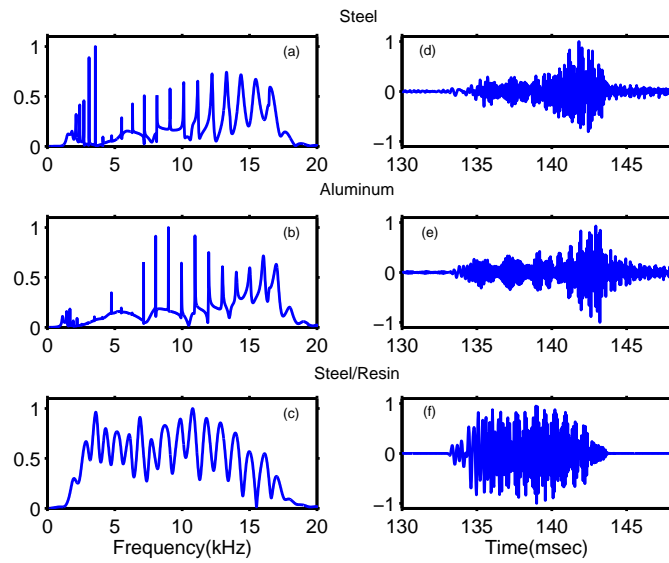


Figure 2: The spectra for the 3 different material types and the echo time series for the 10-ms[2 18] kHz pulse incident upon 5.2% thick shells.

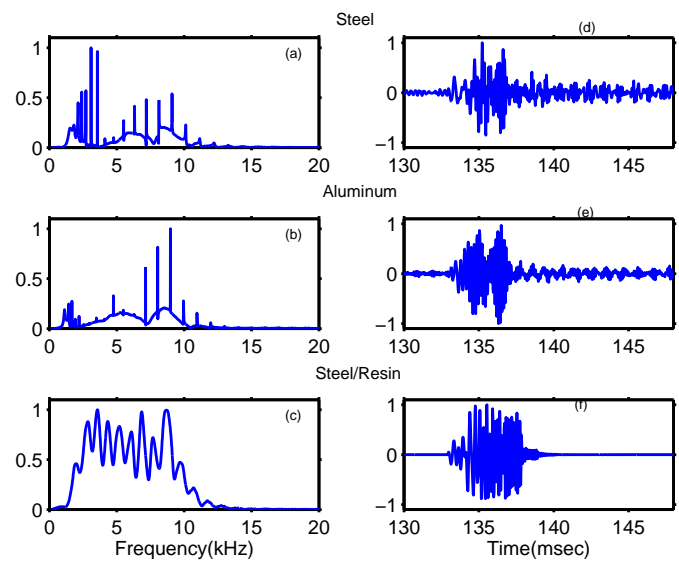


Figure 3: The spectra for the 3 different material types and the echo time series for the 4-ms pulse [2 10]kHz incident upon 5.2% thick shells.

3 CLASSIFICATION PERFORMANCE

3.1 Free space classification of echos

In this section, we consider the classification of echos from spheres in free space. As discussed in the previous section, the echos from a large set of spheres are generated. A portion of these echos will be taken as the “training” set or library and the remainder will comprise the testing set. The echos in the training set will be normalized to have unity L_2 norm. An echo in the testing set will be compared to those in the training set by computing the cross-correlations. We now examine the classification performance for a nearest-neighbour classifier - that is, we consider the sphere in the training set which has the maximum cross-correlation (amplitude of envelope) to yield the class-type of the echo from the testing set. In the first numerical simulation, a random 25% of the spheres’ pulses are used for the training database. Within these signatures, a 510-point (approximately 13 msec) section near the beginning of the echo is extracted. For each pulse in the testing set, 1000-point sections near the beginning of the echos are considered. The cross-correlation operations are performed as a sliding-window, so that the classification is robust to the precise starting time of the echo. We will consider each of the 3 types of spheres subdivided into 2 subclasses: those with relative shell thickness less than or greater than 10%. Thus, there are a total of 6 classes, with Class 1 being thin-shelled, steel (evacuated interior), Class 2, thick-shelled steel (evacuated interior), Class 3, thin-shelled aluminum (evacuated interior), Class 4, thick-shelled aluminum (evacuated interior), Class 5, thin-shelled steel with resin interior and Class 6, thick-shelled steel with resin interior. In this report, we will use Confusion matrices to display the classification results. The (i, j) element of the matrix represents the fraction of times that an object of Class i is classified as belonging to Class j . In Fig.4 we show the Confusion matrices obtained for a 4-fold partitioning of the sphere set into training and testing sets (25% for training, the remainder for testing) using the 10-msec and 4-msec Chirp pulses. As can be seen, the classification results are good for both types of pulse with the 4-msec Chirp pulse yielding somewhat better results. It can be seen from the Confusion matrices that the thick and thin shells are well-discriminated from each other. For example, the steel-shelled sphere may be confused with the aluminum one but there is little confusion between the thick and thin categories. This is why the confusion matrices have a checkerboard appearance.

We now consider the effect of adding noise to the signals of the testing sets. In order to generate a noise sequence related to the incident pulse, we consider a sequence of 20001 point scatterers distributed in range from 90 to 150 m. The phase of each of these scatterers is taken from a smoothed (100 point filter) uniform distribution. The coherent sum is computed for each frequency and weighted by the source spectrum of the incident pulse to produce a reverberation time series. This time series has the same sampling rate as the echo time series and is added to the echo time series.

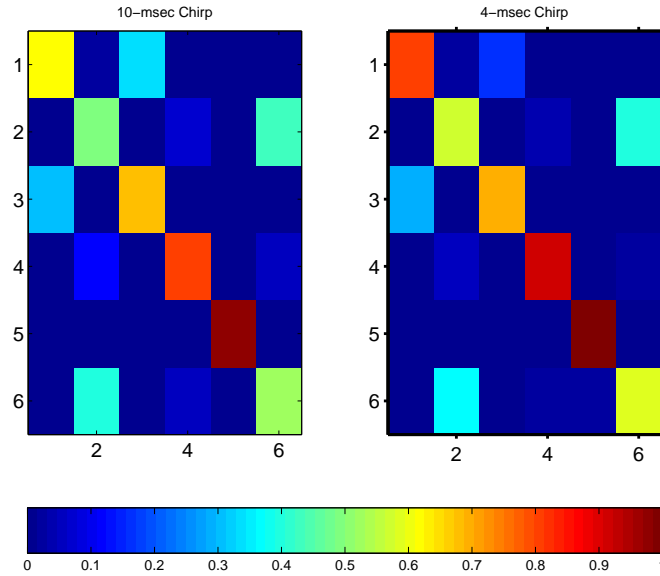


Figure 4: The Confusion matrices resulting from using for the 10-msec and 4-msec Chirp pulses

Example time series for the 10-msec and 4-msec pulses are shown in Fig. 5 for the 5.2% steel-shell. In Fig. 6 we show the corresponding Confusion matrices for the 2 pulses (averaged over 4 partitions) with the noise sequences generated in the same fashion as those shown in Fig. 5. As can be seen, even with significant levels of noise added to the testing sets, the Confusion matrices are very similar to those for the noiseless case shown in Fig. 4. Thus this classification approach of using the cross-correlations of a library of echos with a time series appears to be quite robust with respect to noise (and we have used a noise sequence which lies in the same frequency band as the source). This robustness is not surprising as, for each echo in the training set considered, we are realising some matched-filter gain.

One can also use the classifier to predict the relative shell thickness by simply assigning the relative thickness of the closest signature. A similar estimate of shell thickness from the echo spectra was done in Ref.4 using a kernel-based regression method. In Fig. 7a we show the curves of the predicted relative thickness (logarithm base 10) as a function of the true relative thickness logarithm for the 10 msec pulse and in Fig. 7b we show the same curve when the noise sequence is added to the testing set. The average curves are shown in blue and the red curves show the \pm standard deviations for that particular true value of relative thickness. The relative thickness estimates in Fig.7a are particularly accurate for the true values of the logarithm in the range of about -1 to -.5 and somewhat less precise at the thin and thick values. This is also true for the noise results of Fig. 7b which show a larger standard deviation in the estimated thickness.

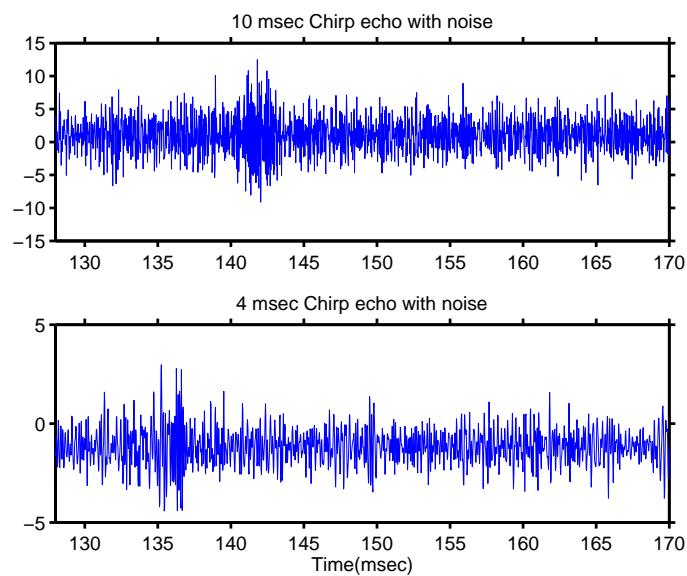


Figure 5: Representative 10-msec and 4-msec Chirp pulse echos with added noise for the 5.2% steel-shelled sphere.

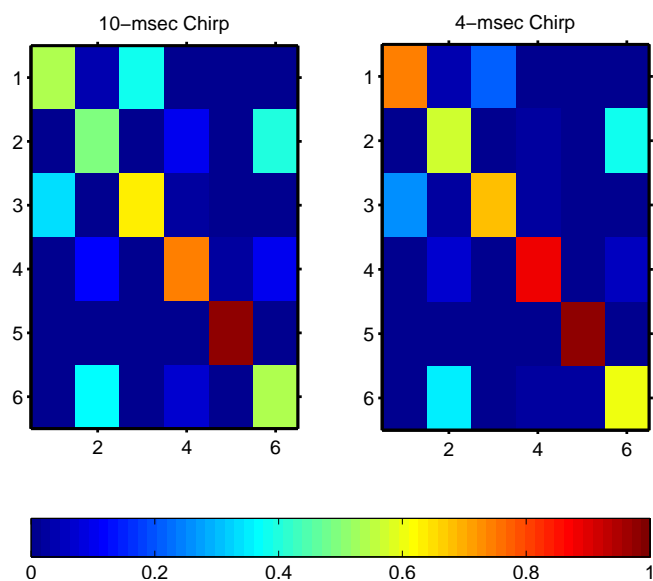


Figure 6: The Confusion matrices resulting from using for the 10-msec and 4-msec Chirp pulses with added noise.

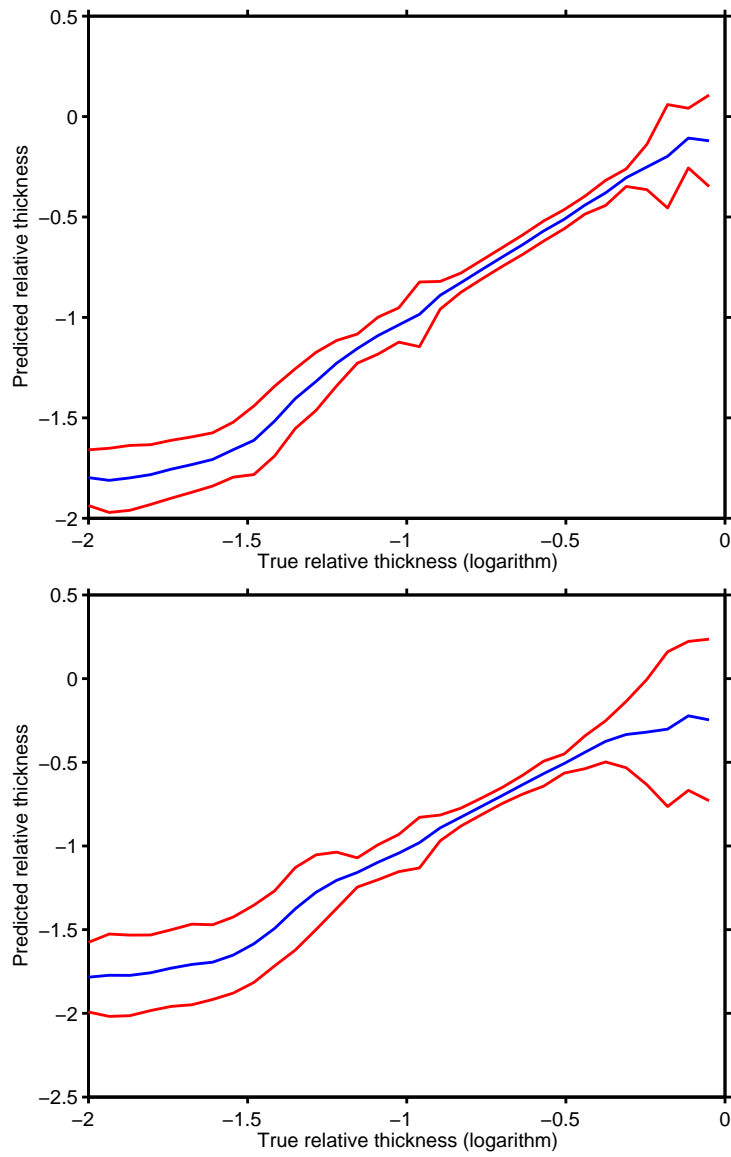


Figure 7: [top] The predicted thickness (logarithm) as a function of the true value. The mean over 4 partitions is shown with the \pm standard deviations also indicated. [bottom] The same as the top plot but noise sequences as in Fig.5 has been added to the testing set

3.2 Classification in a waveguide

We now consider the spheres of the testing set to be in a waveguide. The question is whether they can be successfully classified on the basis of the free space echos or whether the times series in the training set (replicas) must be generated for different hypothesized ranges and depths of the spheres. In Figs. 8 and 9 we show the noiseless time series for a steel-shelled sphere (5% shell) and the same sphere with the resin fill for a 30 m deep waveguide with the source/receiver at 15 m depth. In these figures and for the subsequent results, we consider only the 10 msec Chirp pulse. In Fig.8 the spheres are at a range of 100 m and a depth of 1 m and in Fig. 9 at a depth of 10 m. The time series are shown in the first column and in the second column the results of cross-correlating the waveguide echo with its corresponding free space echo are shown. Some of the multipath arrivals give rise to observable cross-correlation peaks. Other arrivals are not as evident. There are various reasons for the complicated correlation structures. There are pairs of incident and scattered multipath rays at the sphere surface (e.g., direct incidence, surface or bottom reflected path) with a significant angular difference. In these cases, the scattering strength and phase of the echo from the sphere corresponds to a bistatic scattering angle and the corresponding pulse will not correlate perfectly with the freespace (monostatic angle) pulse. Also, the auto-correlation function of the free space echo may have quite significant sidelobes (because the spectrum is far from flat due to the scattering response of the sphere) and this also complicates the cross-correlation structure.

We now consider the classification of the waveguide echos by considering 8 possible depths of the spheres within the waveguide 0.5 m, 1.0 m, 2.0 m, 4.0 m, 10.0 m, 15 m, 20 m and 29.5 m. As above, the source/receiver is in the middle of the waveguide at 15 m depth and a horizontal range of 100 m from the centre of the sphere. For each of these cases we take a random 25% of the free space signatures for the “training” library and the remainder of the indices for the testing set (from the waveguide signatures). The random partitioning is performed twice for each case. “Reverberation” noise of the type discussed for Fig. 5 is added to the testing set. A 500-point section of the free space training signatures are cross-correlated with 1800 points of the testing set starting approximately with the beginning of the echo. The maximum cross-correlation is used to define the classification. The resulting Confusion matrices are shown in Fig. 10. As can be seen, the resulting classifications are quite good for some sphere classes at some of the depths - in particular, at the midwater depths of 10 and 20 m. At the 15 m depth which corresponds to the source/receiver depth, the resulting classification is not as good. This may be due to the fact that the upper surface and seabed reflections exactly overlap in time in this case. For the near surface depths of 1 and 2 m, the classification results are poor. Interestingly, the classifications for the very near surface depth of 0.5 m (and also at 0.5 m off the seabed (depth = 29.5 m)) are better.

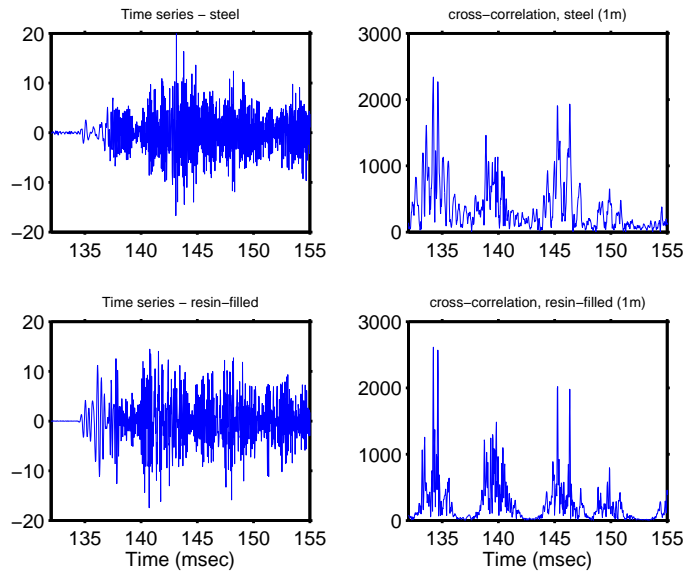


Figure 8: First column: The time series for a steel-shelled (empty) and steel-shelled (resin) at 1 m depth and 100 m range. The source/receiver are at 15m depth in a 30m deep waveguide. Second column: the series resulting from the cross-correlation with the corresponding free-space echo.

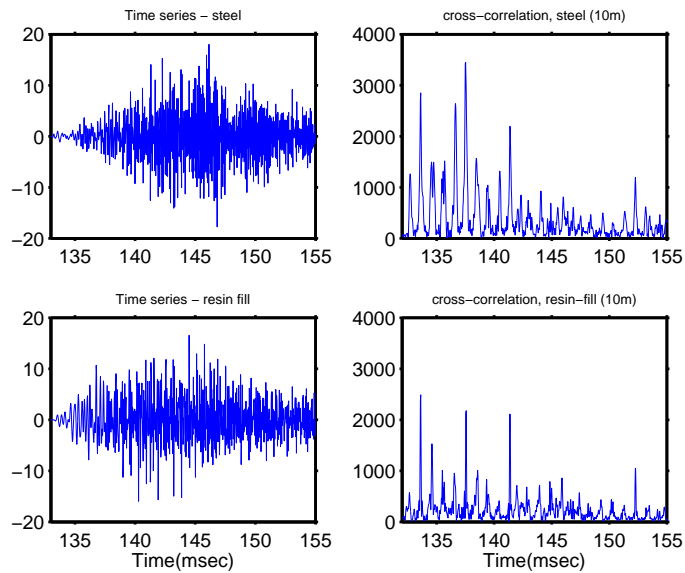


Figure 9: The same as above but now the spheres are at 10m depth.

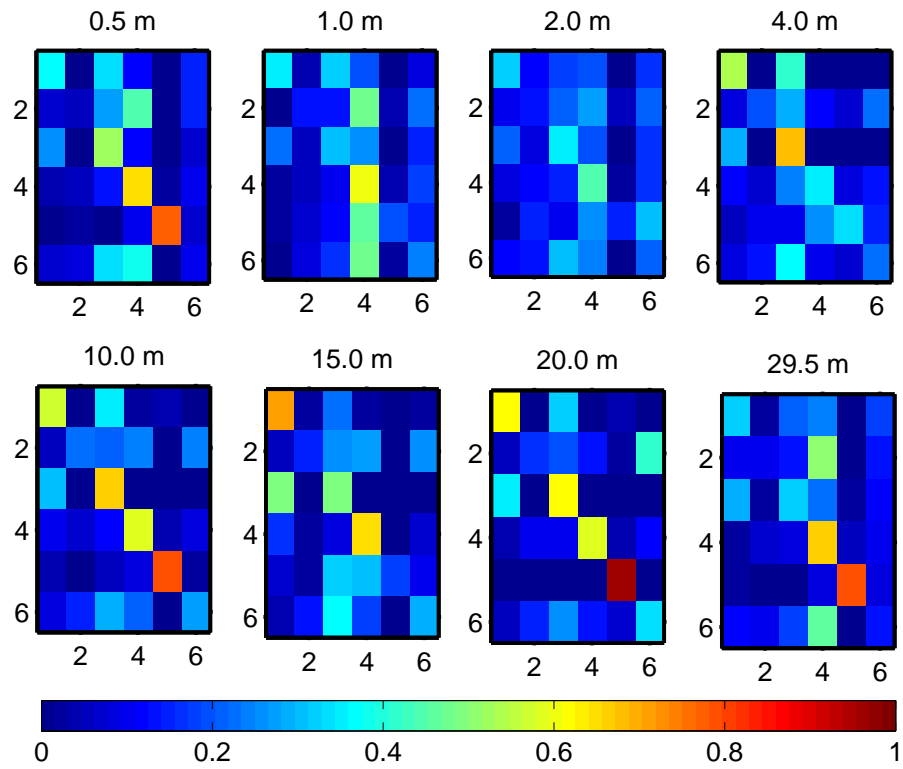


Figure 10: The resulting Confusion matrices for the sphere in a waveguide (30m deep) and for the indicated depths of the spheres. The source/receiver is at 15 m depth and a range of 100 m.

We will now concentrate upon the classification of near surface targets. We will consider a 20 m deep waveguide and ranges of 100 and 200 m. The source/receiver will be at either 1 m below the pressure release surface (i.e., water/air interface) or 1 m above the seabed (i.e., bottom-mounted). The sphere depths are taken to be 0.5 m, 1.0 m, 2.0 m and 4.0 m. In this case, no noise is added to the testing sets and for the training set we use only the odd indices of the free space signatures and for the waveguide testing set the remaining indices. This is the same training/testing partition that was used in Ref. 5. In Figs. 11 and 12 the Confusion matrices for the sphere at 100 m range are shown, first for the source/receiver 1 m deep and then for the source/receiver 1 m off the seabed. In Figs. 13 and 14 the same type of results are shown for the sphere at 200 m range. As can be seen, the classification results are not, in general, good with some exceptions for the 100 m range, particularly for the deep source/receiver.

It is interesting to consider the echos from one of the spheres (10% thick steel-shelled sphere) for the 100 m range for the 2 different source/receiver depths. In Fig. 15 we show the received waveguide echo for the 2 source/receiver depths for the sphere at 2 m depth (from Figs. 11 and 12, it can be seen that the classification results are, in general, poorer for this case for the shallow source/receiver than for the deep source/receiver). There is more of a low frequency component in the deep source/receiver case as destructive interference has nullified the low frequency energy in the shallow case. The corresponding time-frequency plots (using the MATLAB SPECGRAM program) are shown in Fig. 16. As can be seen the energy appears as groups of multipaths for the 2 cases. For example, in the deep source/receiver case, the first linear band corresponds to a combination of direct, surface- and bottom-reflected multipaths. These bands are better separated than in the shallow case and the first arrival group appears to have more energy in the lower frequencies. There is a noticeable band of energy at about 3 kHz, particularly for the shallow source/receiver, corresponding to a resonance in the sphere backscattered spectrum. Due to wrap-around effects in the original time series construction this energy appears as non-causal in the time-frequency plot.

Thus far, we have shown that simply using the free space echos to classify the echos in a waveguide has a mixed classification success dependent upon the range and depth of the object. The question arises as to whether one can classify the sphere accurately if one uses a training set of echos corresponding to the true depth and ranges of the sphere. Also, how accurately does one have to know the target depth and range. In the following figure, we consider the time series for a fixed steel-shelled sphere (radius = 0.3 m, relative thickness = 5.2%) for a range/depth grid of positions within the waveguide and the source/receiver 1 m off the seabed. We then take the echo (800 points) corresponding to range/depth = (100 m, 17 m) and cross-correlate this echo with a set of echos (a 740-point section of the timeseries) from the grid of range, depth positions to form an ambiguity surface which is the left plot in Fig. 17. As can be

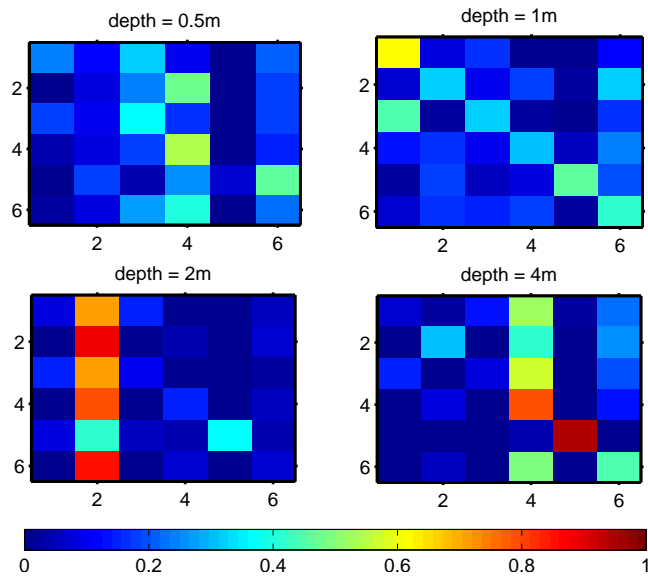


Figure 11: [top] The Confusion matrices for the sphere at 100 m range and the source receiver at 1 m depth. The waveguide depth is 20m.

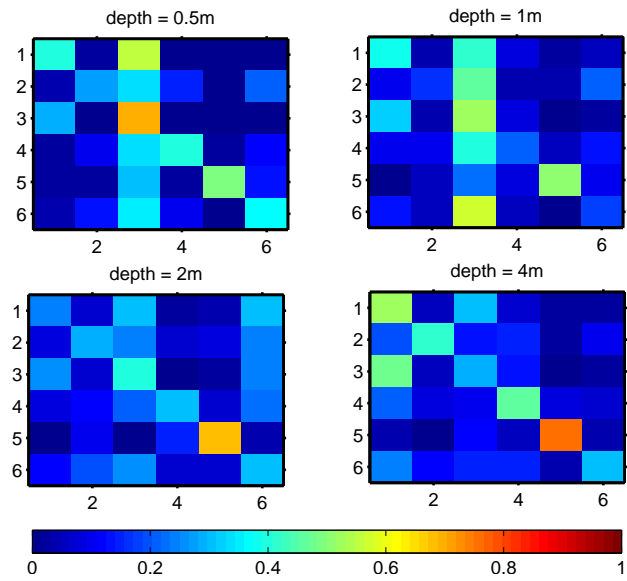


Figure 12: [top] The Confusion matrices for the sphere at 100 m range and the source receiver at 1 m off the seabed. The waveguide depth is 20m.

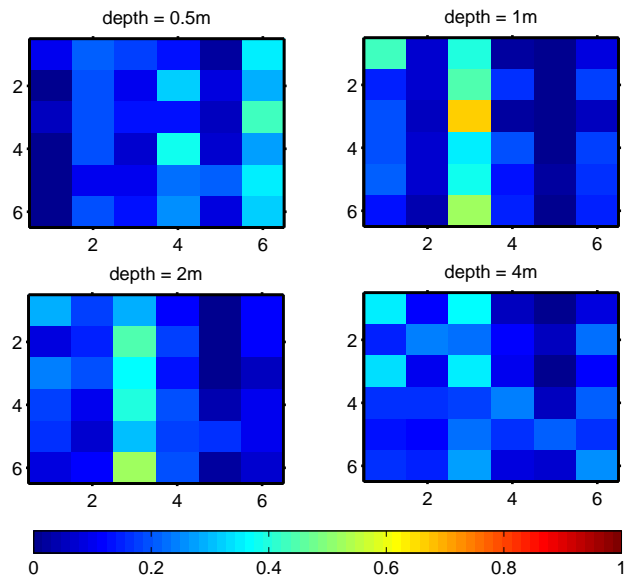


Figure 13: The Confusion matrices for the sphere at 200 m range and the source receiver at 1 m depth. The waveguide depth is 20m.

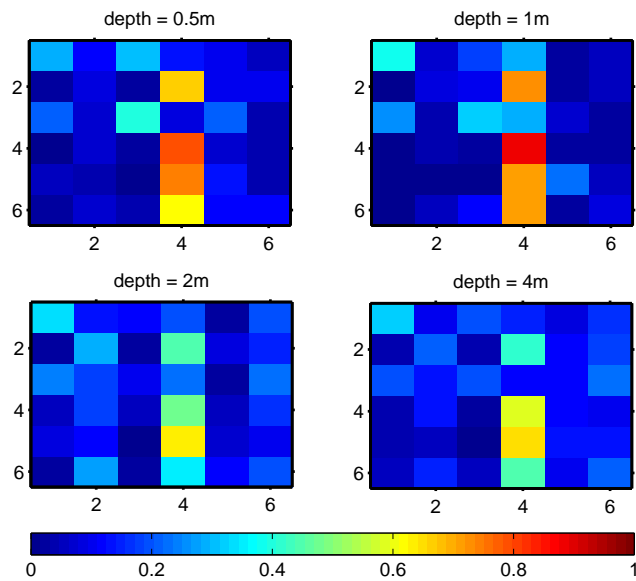


Figure 14: The Confusion matrices for the sphere at 200 m range and the source receiver at 1 m off the seabed. The waveguide depth is 20m.

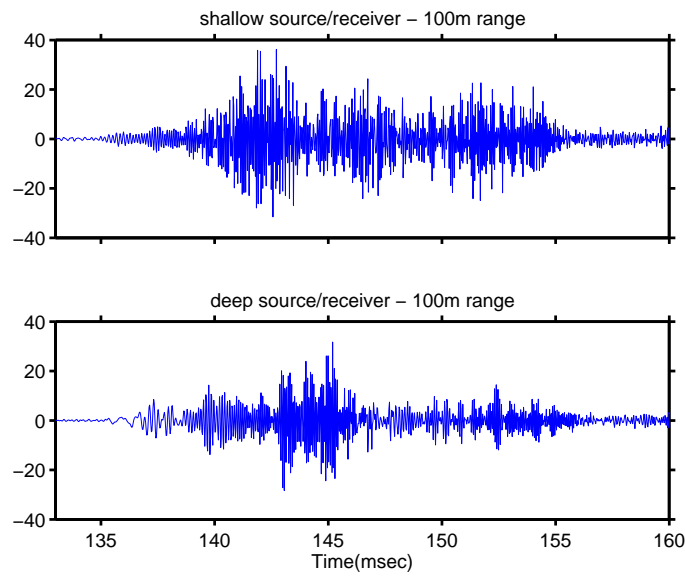


Figure 15: The time series for a steel-shelled (10%) sphere at 100m range and 2m depth for [top] shallow source/receiver [bottom] deep source/receiver

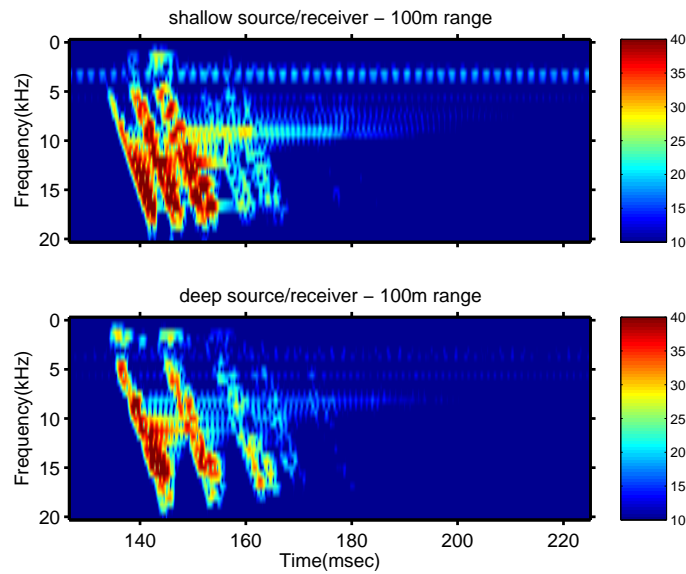


Figure 16: The short time FFT spectra for a steel-shelled (10%) sphere at 100m range and 2m depth for [top] shallow source/receiver [bottom] deep source/receiver. The power is shown in dB units.

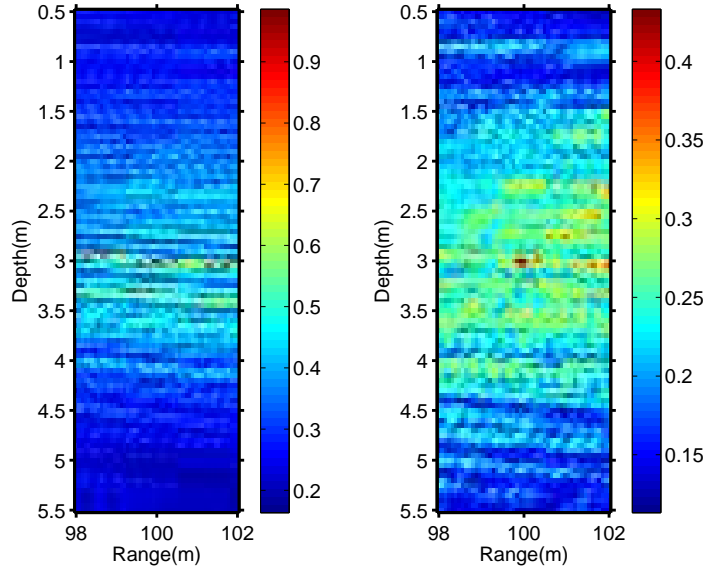


Figure 17: The ambiguity surfaces resulting from cross-correlating a specified echo (at range=100 m, depth = 3 m) with echos from different waveguide positions [left] matching with echos of same type of sphere [right] with echos from different sphere

seen, the cross-correlation falls off rapidly as one moves away from the true depth and less so with respect to range. Thus, it is interesting to note that from a knowledge of the sphere type one can, in fact, localize the target by optimizing the cross-correlation function. In the right panel of Fig. 17, we show the resulting ambiguity surface when one cross-correlates with the waveguide echos from a solid (approximately), steel-shelled sphere with a radius of 0.27 m (i.e., the matching sphere is incorrect). The level of cross-correlation is significantly lower but the estimated location is correct. In general, we have noted that the location parameters of the target can be determined quite rapidly on the basis of optimizing the cross-correlation with even incorrect sphere signatures.

We now investigate whether, given a discrete set of sphere sizes, thicknesses and types, one can successfully classify waveguide echos by first generating waveguide echos for the training set of sphere. The ranges and depths considered will span the true target location. In order to reduce the amount of computation time we fix the horizontal range at its true value. In practice, for an active sonar, the range can be fairly well estimated from the round-trip travel time. There are 2 basic ways that we can generate the replicas for different hypothesized depths. Let us suppose that we have the free space monostatic echo or free space monostatic scattering spectrum $F(\omega)$. For a source/receiver depth z_r and the sphere centre at range r and depth z_s , there are scattering angles at the sphere associated with each incident/scattered multipath combination. We will assume that for each pair of incident/scattered ray paths angles

that we can simply multiply the 2-way propagation term by $F(\omega)$. Summing over all the multipath pairs, we can compute at each frequency a scalar term (independent of the sphere) with which to multiply a sphere's monostatic scattering function $F(\omega)$. The significant approximation which has been made is that the true bistatic scattering function $F(\omega : \Delta\phi)$ has been approximated with $F(\omega, \Delta\phi = 0)$. This monostatic approximation may be good in the case that the first target echos correspond to small scattering angles. The second more accurate approach is to store (or compute on the fly) the scattering coefficients $a_n(\omega)$, $n = 1, \dots, N$ for each sphere of the training set as a function of frequency. Alternatively, one could store an angularly-dependent scattering function for each frequency and use interpolation for arbitrary values of the scattering angle. From the scattering coefficients, the exact angular scattering pattern can be computed at each frequency and for each incident/scattered multipath pair at the sphere, one can apply the correct scattering factor. The advantage of the first approach is that it requires less storage (simply the free space echos which are quickly converted) and one can, in fact, use experimentally measured echos. In the second approach, if one wished to use experimental data for the training set, then measurements of the echos at various bistatic angles would be required. The angular discretization would need to be fine enough, so that in the multipath model, interpolation could be accurately used for an arbitrary scattering angle,

We now repeat the computations for the Confusion matrices of Figs. 11–14 but generating replicas for hypothesized depths spanning the true depth of the target. In addition, we add noise of the levels used in the free space classification. We first use the monostatic approximation to compute at each depth and frequency a scaling factor to apply to $F(\omega)$. The depth discretization used is 10 cm and the true depth is 5 cm away from the nearest 2 indices. For example, for a true depth of 19 m, the search window used is [18.45 19.45]m with 11 increments of 10 cm. For each echo in the testing set, the echo and the depth in the training set which yields the maximum cross-correlation, is used to give the class. The resulting Confusion matrices are shown in Figs.18-19 for the spheres at 100 m range and shallow and deep source/receiver depths and, similarly, in Figs.20-21 for the spheres at 200 m range. As can be seen, the method has, in general, improved the classification results from simply using the free space echos for classification. It has worked particularly well for the deep source (1 m off the seabed) for both the 100 and 200 m ranges. This may be due to the geometry and the coherent interference of the multipaths. In the case of the near surface targets and the near source source, the travel time (or phase) difference between the direct and surface reflected paths is very small (.013 msec in the case of the sphere at 1 m depth and 100 m range). Thus, the combined direct and surface-reflected echo is very small in amplitude, particularly the leading portion corresponding to the lower-frequencies. After about 5 msec, the direct/bottom bounce and surface/bottom bounce paths arrive. In this case, the scattering angle at the sphere is approximately 21° and the monostatic approximation may not be good.

For the bottom source/receiver, the direct, surface, and bottom reflected paths to and from the sphere arrive in a group but the time difference between the direct and subsequent arrivals is about 0.25 msec and for all the multipaths in this group the scattering angle at the sphere is small.

Finally, we consider constructing the exact, multipath replicas for the case of the sphere at 1 m depth and 100 m horizontal range and the source/receiver at 1 m depth. This is a case where the classification results were still somewhat poor after using the monostatic-generated replicas. The depths are searched in the interval [18.45 19.45]m in 11 steps of 0.1m. The horizontal range is set to its true value. Thus, there are 2 depths, 18.95 m and 19.05 m, within 5 cm of the true depth (of course, since the maximum correlation value is chosen, the depth may, in some case, be relatively far from the correct depth value). In this case, the frequency-dependent scattering coefficients are used for each sphere type of the “training” set to generate a replica vector at each depth which computes the correct angularly-dependent scattering function to use in conjunction with the multi-path expansion. The resulting Confusion matrix is shown in Fig. 22. The classification results are better than in Fig. 18 where the simplified (monostatic) replica method was used.

4 SUMMARY

We have investigated in this report the effect of the waveguide on the simple correlation classification of targets. The modeling of the scattering from a spherically-shelled target in a waveguide used the multipath expansion method described in Ref.7. The approach of this paper for classification is very straightforward. The “feature” set is the echo (or some portion of it) and the running cross-correlations of a set of training echos with this echo provides the classification. For the object classes and sonar pulse considered, it was possible to quite accurately classify the 6 object types in free space from this “library” of echos. This simple classification scheme was robust in the presence of a significant amount of added noise. When the spheres were placed within a shallow oceanic waveguide, the accurate classification of the objects using a set of free space echos was possible at some ranges and depths. In particular, at 100 m range and at the depth where the direct and various multipath arrivals were sufficiently separable, the resulting classifications were good. When the sphere was close to one of the interfaces, so that there is significant cancellation of portions of the direct echo, the classifications using free space echos may be poor. We considered improving the classification by using a training set of echos generated for the waveguide and spanning the range and depth of the sphere. A generated ambiguity surface showed that, in fact, the amplitude of the coherent cross-correlation between a sphere’s echo and the corresponding echos at different waveguide positions falls off rapidly from the true location. However, it may be possible to estimate the sphere’s location rapidly

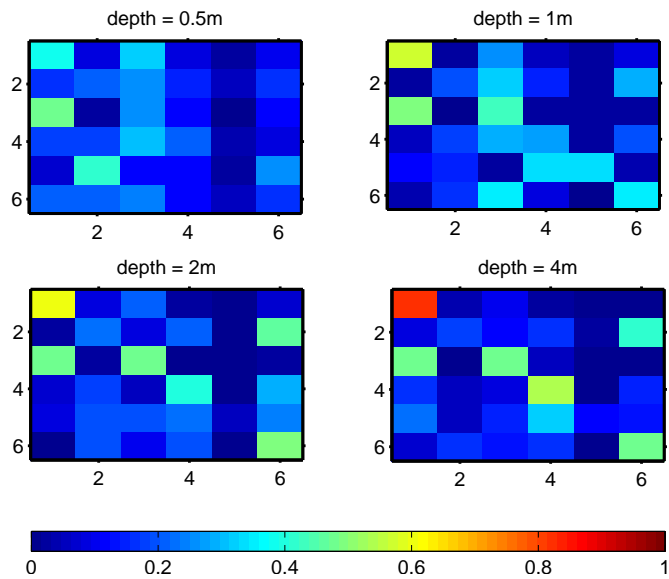


Figure 18: The Confusion matrices for the sphere at 100 m range and the source receiver at 1 m depth. Eleven replicas are generated for depths bracketing the true depth and the maximum cross-correlation is used.

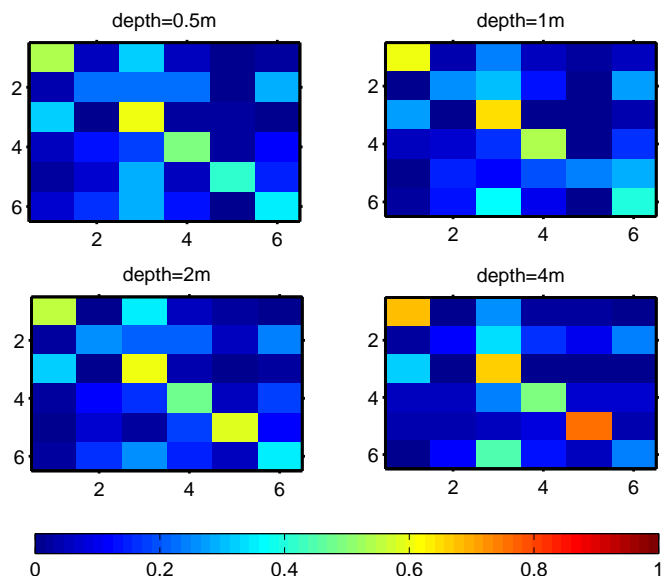


Figure 19: The Confusion matrices for the sphere at 100 m range and the source receiver at 1 m off the seabed. Eleven replicas are generated for depths bracketing the true depth and the maximum cross-correlation is used.

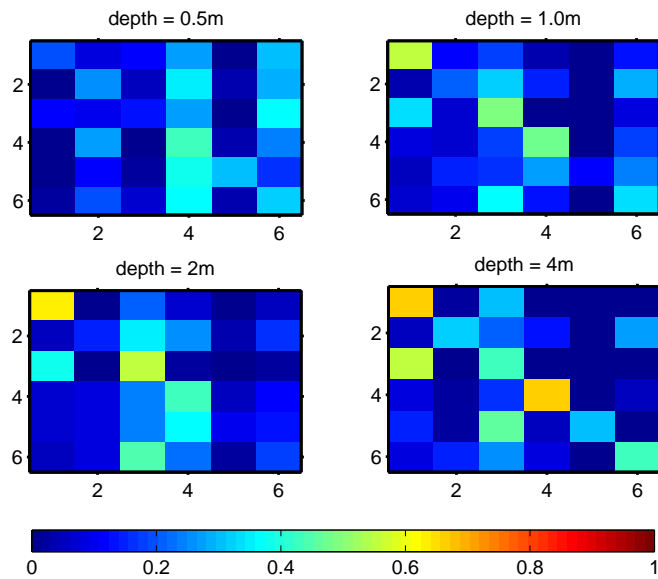


Figure 20: The Confusion matrices for the sphere at 200 m range and the source receiver at 1 m depth. Eleven replicas are generated for depths bracketing the true depth and the maximum cross-correlation is used.

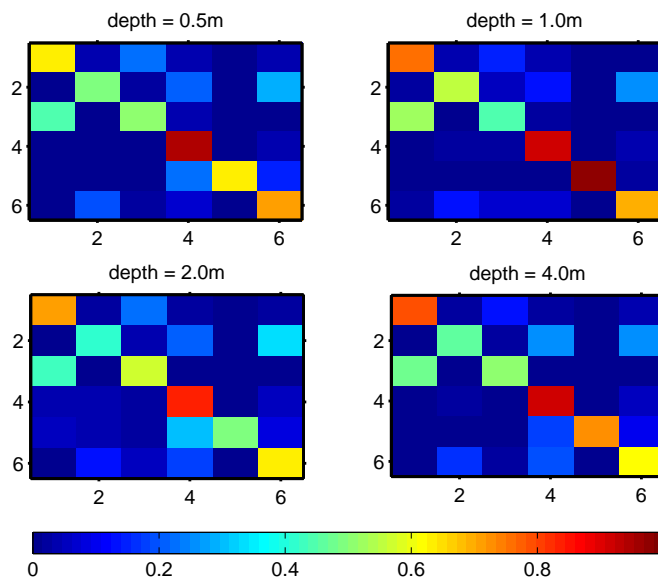


Figure 21: The Confusion matrices for the sphere at 200 m range and the source receiver at 1 m off the seabed. Eleven replicas are generated for depths bracketing the true depth and the maximum cross-correlation is used.

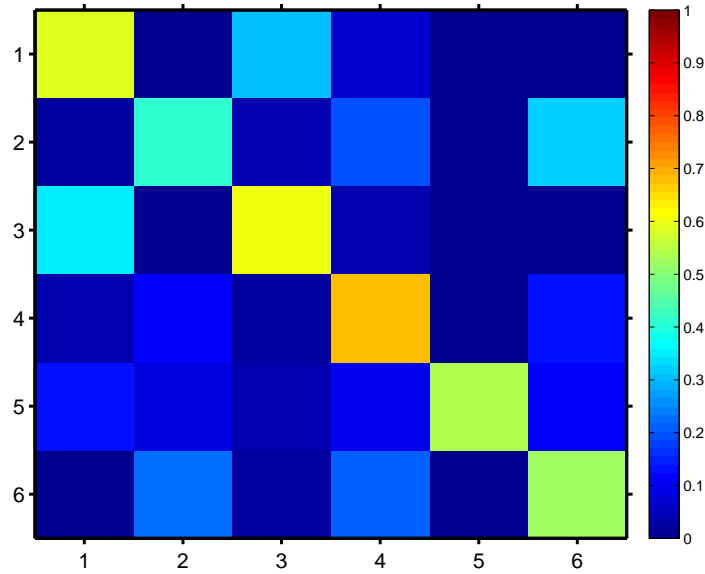


Figure 22: The resulting Confusion matrix for the sphere at 100 m range and 1 m depth. The source/receiver is at 1 m depth. The depth of the sphere is searched over the interval [18.45 19.45]m

by using only a few of the hypothesized spheres in the training set. We considered generating waveguide echos for the spheres of the training set in 2 different ways. The simpler, more efficient approach was to compute a frequency-dependent scalar with which to multiply the spheres' monostatic free space scattering function. The same frequency scaling factors can be applied to all the spheres. This is expected to be most accurate when the scattering angles at the sphere are small. This approach was found to be quite effective for shallow targets when the source/receiver was close to the seabed. It did not work as well for the source/receiver and the sphere both at shallow water depths. Finally, we showed the resulting Confusion matrix when a full angular-dependent scattering computation was done as a function of sphere depth when generating replica vectors for the training set. In this case, the spheres were at a range of 100 m and a depth of 1.0 m with the source/receiver also at 1 m depth. The resulting classifications were quite good.

The approach considered in this paper could be extended in a number of ways. One could consider the effects of beamforming at the source and/or receiver in order to mitigate some of the multipath effects. The effects of using multiple source/reciver pairs could be investigated. As well, there could be classification improvements if a multiple echo/tracking approach was used. The use of even wider band pulses could improve classification performance. We have considered the problem from a classification perspective - we have used spherical targets to simplify the modelling. A fixed set of spheres was considered as the training set or to define the set of scattering

coefficients to use in the sphere/waveguide modelling. In the case where the free space monostatic echos were used, either directly or modified by the waveguide, the same approach could be used for a training set of measurements for more general targets. In the case, where the set of scattering coefficients was used, one would have to measure a sufficiently sampled set of bistatic echos. The other approach which could be used in the case of spherical targets is to use an inversion technique (to jointly estimate spherical/location parameters).

There are, of course, other temporal, spectral and temporal/spectral features which could be used for classification. However, it is expected that waveguide propagation would certainly have an effect in these cases as well. The method of this paper presents an useful baseline performance for classification in free space and for targets in a waveguide.

References

- [1] D.D. Sternlicht, A.W. Thompson, D.W. Lemonds, R.D. Dikeman, and M.T. Korporaal, "Image and signal classification for a buried object scanning sonar", in *Proceedings of IEEE/MTS Oceans 2002*, Vol.1, pp.485-490, (2002).
- [2] F.B. Shin, D.H. Kil, and R.F. Wayland, "Active impulsive echo discrimination in shallow water by mapping target physics-based features to classifiers", *IEEE Journal of Oceanic Engineering*, Vol.22, pp.66-80, 1997.
- [3] H.Liu, P. Runkle, L. Carin, T. Yoder, T. Giddings, L. Couchman and J. Bucaro, "Classification of distant targets situated near channel bottoms", *J. Acoust Soc.*, Vol. 115, pp. 1185–1197 (2004).
- [4] J. Sildam and J. Fawcett, "Baseline classification of acoustical signatures of mine-like objects", DRDC Atlantic TM 2005-058, July 2005.
- [5] J.A. Fawcett, W.L.J. Fox, and A. Maguer, "Modeling of scattering by objects on the seabed", *J. Acoust. Soc. Am.*, Vol. 104, pp.3296-3304 (1998).
- [6] J.A. Fawcett, "Broadband scattering from spherical shells in a waveguide: modeling and classification", in *Proceedings of Acoustics'08, Paris, 2008*
- [7] J.A. Fawcett, "Modelling broadband scattering from shelled spheres in a waveguide", DRDC Atlantic TM 2007-270, October 2007.
- [8] W.G. Neubauer, *Acoustic reflection from surfaces and shapes*, Naval Research Laboratory, Washington, D.C., U.S.A., 1986.

- [9] A. Tesei, P. Guerrini, and M. Zampolli, "Tank measurements of elastic scattering by a resin-filled spherical shell", in *Proceedings of Underwater Acoustic Measurements: Technologies and Results*, F.O.R.T.H, Heraklion, Crete, Greece, 2007.
- [10] J.A. Fawcett, "Modelling of high-frequency scattering from elastic spheres", DREA TM 98-233, February, 1999.
- [11] G.S. Sammelmann and R.H. Hackman, "Acoustic scattering in a homogenous waveguide", *J. Acoust. Soc. Am.*, Vol.82, pp.324-336, 1987.
- [12] R.H. Hackman and G.S. Sammelmann, "Multiple-scattering analysis for a target in an oceanic waveguide", *J. Acoust. Soc. Am.*, Vol.84, pp. 1813-1825, 1988.
- [13] N.C. Makris, "A spectral approach to 3-D object scattering in layered media applied to scattering from submerged spheres", *J. Acoust. Soc. Am.*, Vol.104, pp.2105-2113, 1998.
- [14] Y. Lai and N.C. Makris, "Spectral and modal formulations for the Doppler-shifted field scattered by an object moving in a stratified medium", *J. Acoust. Soc. Am.*, Vol. 113, pp.223-244, 2003.
- [15] K.V. Rao, N.M. Kee, P.W. Goalwin, and H. Schmidt, "Element level simulation of sonar echo from a moving target in an ocean waveguide", in *Proceedings of IEEE/MTS Oceans 94*, Vol.3, pp. 195-199, 1994.
- [16] G.V. Frisk, *Ocean and seabed acoustics: A theory of wave propagation*, PTR Prentice Hall, 1994.
- [17] F. Ingenito, "Scattering from an object in a stratified medium", *J. Acoust. Soc. Am.*, Vol. 82, pp.2851-2859 (1987).
- [18] E.K. Westwood and C.T. Tindle, "Shallow water time-series simulation using ray theory", *J. Acoust. Soc. Am.*, Vol.61, pp. 1752-1761, 1987.

This page intentionally left blank.

Distribution list

DRDC Atlantic TM 2008-217

Internal distribution

- 1 Mae Seto, GL/MHD
- 1 Dave Hazen, SH/TD
- 1 Mark Trevorrow, GL/TorD
- 1 John Fawcett
- 1 Juri Sildam
- 5 Library

Total internal copies: 10

External distribution

- 1 NDHQ/DRDKIM
- 1 Library and Archive Canada

Total external copies: 2

Total copies: 12

This page intentionally left blank.

DOCUMENT CONTROL DATA

(Security classification of title, body of abstract and indexing annotation must be entered when document is classified)

1. ORIGINATOR (The name and address of the organization preparing the document. Organizations for whom the document was prepared, e.g. Centre sponsoring a contractor's report, or tasking agency, are entered in section 8.) Defence R&D Canada – Atlantic P.O. Box 1012, Dartmouth, Nova Scotia, Canada B2Y 3Z7		2. SECURITY CLASSIFICATION (Overall security classification of the document including special warning terms if applicable.) UNCLASSIFIED	
3. TITLE (The complete document title as indicated on the title page. Its classification should be indicated by the appropriate abbreviation (S, C or U) in parentheses after the title.) Broadband classification of spherical shells in a waveguide			
4. AUTHORS (Last name, followed by initials – ranks, titles, etc. not to be used.) Fawcett, J.A.; Sildam, J.			
5. DATE OF PUBLICATION (Month and year of publication of document.) November 2008	6a. NO. OF PAGES (Total containing information. Include Annexes, Appendices, etc.) 42	6b. NO. OF REFS (Total cited in document.) 18	
7. DESCRIPTIVE NOTES (The category of the document, e.g. technical report, technical note or memorandum. If appropriate, enter the type of report, e.g. interim, progress, summary, annual or final. Give the inclusive dates when a specific reporting period is covered.) Technical Memorandum			
8. SPONSORING ACTIVITY (The name of the department project office or laboratory sponsoring the research and development – include address.) Defence R&D Canada – Atlantic P.O. Box 1012, Dartmouth, Nova Scotia, Canada B2Y 3Z7			
9a. PROJECT NO. (The applicable research and development project number under which the document was written. Please specify whether project or grant.) 11CF	9b. GRANT OR CONTRACT NO. (If appropriate, the applicable number under which the document was written.)		
10a. ORIGINATOR'S DOCUMENT NUMBER (The official document number by which the document is identified by the originating activity. This number must be unique to this document.) DRDC Atlantic TM 2008-217	10b. OTHER DOCUMENT NO(s). (Any other numbers which may be assigned this document either by the originator or by the sponsor.)		
11. DOCUMENT AVAILABILITY (Any limitations on further dissemination of the document, other than those imposed by security classification.) (X) Unlimited distribution () Defence departments and defence contractors; further distribution only as approved () Defence departments and Canadian defence contractors; further distribution only as approved () Government departments and agencies; further distribution only as approved () Defence departments; further distribution only as approved () Other (please specify):			
12. DOCUMENT ANNOUNCEMENT (Any limitation to the bibliographic announcement of this document. This will normally correspond to the Document Availability (11). However, where further distribution (beyond the audience specified in (11)) is possible, a wider announcement audience may be selected.)			

13. **ABSTRACT** (A brief and factual summary of the document. It may also appear elsewhere in the body of the document itself. It is highly desirable that the abstract of classified documents be unclassified. Each paragraph of the abstract shall begin with an indication of the security classification of the information in the paragraph (unless the document itself is unclassified) represented as (S), (C), (R), or (U). It is not necessary to include here abstracts in both official languages unless the text is bilingual.)

In this paper, a multipath expansion method is used to model the scattering from a large set of spheres in a Pekeris waveguide. The spherical shells have different radii, relative thicknesses, and three different materials and are grouped into 6 classes: thick and thin-shelled and 3 different material compositions. The classification of the spheres from their echos is considered, first for the sphere in free space and then for the spheres in the waveguide. The cross-correlations of the observed echos with a library of echos is the basis of the classification. In the case of echos from a sphere in a waveguide, we consider the resulting classifications when using a library of free space echos and then echos modified with increasing accuracy to account for the waveguide propagation. The cross-correlation based classification approach has been chosen because of its common use in sonar target detection applications. It is hoped that the present results can be used as an intuitive baseline for the development of other target/waveguide classification methods.

14. **KEYWORDS, DESCRIPTORS or IDENTIFIERS** (Technically meaningful terms or short phrases that characterize a document and could be helpful in cataloguing the document. They should be selected so that no security classification is required. Identifiers, such as equipment model designation, trade name, military project code name, geographic location may also be included. If possible keywords should be selected from a published thesaurus. e.g. Thesaurus of Engineering and Scientific Terms (TEST) and that thesaurus identified. If it is not possible to select indexing terms which are Unclassified, the classification of each should be indicated as with the title.)

sphere, waveguide, scattering

This page intentionally left blank.

Defence R&D Canada

Canada's leader in defence
and National Security
Science and Technology

R & D pour la défense Canada

Chef de file au Canada en matière
de science et de technologie pour
la défense et la sécurité nationale



www.drdc-rddc.gc.ca